Environmental Pollution 298 (2022) 118808

Contents lists available at ScienceDirect

Environmental Pollution

journal homepage: www.elsevier.com/locate/envpol

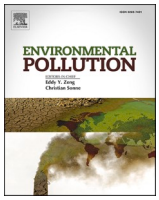

Microplastic variability in subsurface water from the Arctic to Antarctica☆

Svetlana Pakhomova [a,b,*], Anfisa Berezina [b,c], Amy L. Lusher [a,d], Igor Zhdanov [b], Ksenia Silvestrova [b], Peter Zavialov [b], Bert van Bavel [a], Evgeniy Yakushev [a,b,e]

[a] Norwegian Institute for Water Research, Oslo, Norway
[b] P.P. Shirshov Institute of Oceanology, Russian Academy of Sciences, Moscow, Russia
[c] St. Petersburg State University, Saint Petersburg, Russia
[d] Department of Biological Sciences, University of Bergen, Norway
[e] V.I.Il'ichov Pacific Oceanological Institute, Far Eastern Branch of the Russian Academy of Sciences, Vladivostok, Russia

ARTICLE INFO

Keywords:
Microplastic
Global distribution
Subsurface water
Fibers
Harmonization

ABSTRACT

Comparative investigations of microplastic (MP) occurrence in the global ocean are often hampered by the application of different methods. In this study, the same sampling and analytical approach was applied during five different cruises to investigate MP covering a route from the East-Siberian Sea in the Arctic, through the Atlantic, and into the Antarctic Peninsula. A total of 121 subsurface water samples were collected using underway pump-through system on two different vessels. This approach allowed subsurface MP (100 μm–5 mm) to be evaluated in five regions of the World Ocean (Antarctic, Central Atlantic, North Atlantic, Barents Sea and Siberian Arctic) and to assess regional differences in MP characteristics. The average abundance of MP for whole studied area was 0.7 ± 0.6 items/m^3 (ranging from 0 to 2.6 items/m^3), with an equal average abundance for both fragments and fibers (0.34 items/m^3). Although no statistical difference was found for MP abundance between the studied regions. Differences were found between the size, morphology, polymer types and weight concentrations. The Central Atlantic and Barents Sea appeared to have more MP in terms of weight concentration (7–7.5 μg/m^3) than the North Atlantic and Siberian Arctic (0.6 μg/m^3). A comparison of MP characteristics between the two Hemispheres appears to indicate that MP in the Northern Hemisphere mostly originate from terrestrial input, while offshore industries play an important role as a source of MP in the Southern Hemisphere. The waters of the Northern Hemisphere were found to be more polluted by fibers than those of the Southern Hemisphere. The results presented here suggest that fibers can be transported by air and water over long distances from the source, while distribution of fragments is limited mainly to the water mass where the source is located.

1. Introduction

Contamination of the global environment by microplastic (MP) is receiving worldwide attention, with national and international efforts driven by a common goal to understand the fate and risk of these anthropogenic pollutants. Researchers have applied many different sampling and analytical approaches to begin to quantify abundances of MP. It is challenging to compare the generated data when different methodological approaches have been applied (Cowger et al., 2020). As an example, some approaches rely on visual identification, without analytical chemistry confirmation that the particles are plastic. In other cases, researchers report values as number per unit volume/area, or mass per unit volume/area (Campos da Rocha et al., 2021). In many cases, the criteria for including or excluding particles are researcher and project specific (Brander et al., 2020). Furthermore, some of these approaches have limitations related to the reproducibility of the methodological approach, controlling for procedural contamination, and including adequate quality control and quality assurances (Brander et al., 2020; Provencher et al., 2020).

Harmonized and validated approaches are being recommended for collecting comparable data within monitoring programmes (GESAMP, 2019; Michida et al., 2019; Odland et al., 2016). When plastic pollution research started to look at surface waters much of the information gathered utilised neuston nets (e.g., Law et al., 2010; Moore, 2008) and

☆ This paper has been recommended for acceptance by Eddy Y. Zeng.

* Corresponding author. Norwegian Institute for Water Research, Oslo, Norway.
E-mail address: svp@niva.no (S. Pakhomova).

https://doi.org/10.1016/j.envpol.2022.118808
Received 7 October 2021; Received in revised form 28 December 2021; Accepted 5 January 2022
Available online 7 January 2022

focused on the larger, visible fraction of plastics (>300 μm). This has suported harmonization and validation of data obtained using Manta, or similar neuston nets. However, net sampling has drawbacks which include the size of particles captured, a high risk of procedural contamination and the exclusion of fibers from total counts (Cózar et al., 2014; Isobe et al., 2021). Furthermore, sampling by nets is also affected by the weather and biotic conditions. Net sampling is reliant on calm waters, little wind and low biological activity; the method works best when applied in enclosed coastal locations. Similarly, the cost of deploying multiple trawls and slowing research vessels can limit the scale at which assessments of MP contamination are conducted. Whilst the influence of coastal currents and regional dynamics are interesting (Chubarenko et al., 2018), MP concentrations, their transport, and distribution in offshore waters is targeted by research to look at the large-scale impacts of oceanographic processes (Sebille et al., 2020). Similarly, scientific advances in methodological approaches are encouraged to focus on the smaller size fraction of MP <300 μm and optimising these processes with minimum procedural contamination. The smaller particles are of interest as they are likely to have the biggest impact on ecosystems, especially biota (Covernton et al., 2019). To facilitate this, researchers began to investigate the use of vessels of opportunity to support research of MP contamination in the ocean surface water (O'Conchubhair et al., 2019; Kanhai et al., 2017; Lusher et al., 2014; Morgana et al., 2018; Ross et al., 2021). Here, a seawater intake is utilised to collect surface and subsurface water. Pumping of subsurface water for MP has become a favourable method as it is possible to cover the vast expanses of the ocean that doesn't require additional shiptime and it allows the study of smaller MP, down to 10 μm. Research on smaller MP requires a higher level of quality control and assurance, which includes confirmation particles are plastics, and contamination control. Depending on the different approaches used for sampling and analysis, this can significantly affect the calculated oncentrations of MP.

Accurately and efficiently reporting MP data in the ocean surface will support the risk assessment of MP to pelagic ecosystems. At the same time, collecting real-time data on MP abundance in the global oceans is necessary to validate the accuracy of numerical modelling (Van Sebille et al., 2015). Model studies often consider plastic as a passive tracer, disregarding the processes of fragmentation, decomposition, and biofouling. Biofouling has only recently been introduced as a topic when modelling MP distribution (Berezina et al., 2021; Lobelle et al., 2021).

To date, there are several datasets generated on plastics and MP abundance, however these datasets focus on the larger fraction of plastics. As an example (Eriksen et al., 2014), compiled data from 680 surface net tows collected between 2007 and 2013, with the data standardised to reduce uncertainty from oceanic conditions (vertical mixing, turbulence etc.). Similarly (Cózar et al., 2014), synthesized MP abundance data obtained from 841 surface net tows (442 wind-corrected samples) and Van Sebille et al. (2015) utilised a similar approach for 11,632 samples from 1979 to 2013. Most of MP studies in seawater deal with floating items only, which is not enough to draw a full picture of MP fate in the ocean. Isobe et al. (2021) provided a new dataset of pelagic MP abundance in the world's oceans which incorporates different sampling methods. The authors considered 8,218 pelagic MP samples from 2000 to 2019. It is evident that without special data processing to account for the many variations in methodological approach, it is challenging to compare the results from different regions (Table 1).

In this study we used a harmonized technique, from sampling to data reporting, to collect data of MP in subsurface water from five different cruises covering a route from the East-Siberian Sea in the Arctic through the Atlantic to the Antarctic. The goal of this work was to compare the pollution of subsurface water with MP in different regions of the World Ocean and to identify patterns of MP distribution that can help to understand MP fate in the ocean.

2. Methods

2.1. Study area

Floating microdebris from the upper mixed layer (about 3 m depth) were sampled along a transect Tromsø-Svalbard onboard cargo vessel *Nordbjørn* in August 2019 and during four research cruises of R/V *Akademik Mstislav Keldysh* in September 2019–February 2020 to the East Siberian, Laptev, Kara, Barents, Norwegian, and North Seas, Central/South Atlantic Ocean, and in the Scotia Sea down to the Antarctic (Fig.1).

According to the Global Ocean circulation patterns (Emery, 2001; Rudels, 1989; Rudels et al., 2004), the study area can be divided into five regions, namely: (i) Antarctic (south of 40°S); (ii) Central Atlantic (between 35°S and 35°N); (iii) North Atlantic (along Norwegian coast to 20°E and north to Svalbard); (iv) Barents Sea (east of 20°E to the western Kara Sea, 65°E); and (v) Siberian Arctic (east of 65°E). Regions (i-iii) belong to the Atlantic Ocean water. The Antarctic region here includes two water masses: Sub Antarctic Surface Water (SASW) and Antarctic Surface Water (AASW) which could be considered as circumpolar surface waters (Emery, 2001). In the Central Atlantic region stations belong mainly to the South Atlantic Central Water (SACW) and only two northern stations – belonging to the Eastern North Atlantic Central Water (ENACW) (Emery, 2001). The North Atlantic region is represented by stations along the North Atlantic Current and referred to the Atlantic Subarctic Upper Water (ASUW). Both the Barents Sea and Siberian Arctic regions belong to the Arctic Ocean water. The water of the Barents Sea penetrates the Kara Sea until it reaches the plume of the Ob River. The border between the Barents Sea and Siberian Arctic regions

Table 1
Studies of subsurface MP in different regions with different variation of sampling and analysis.

Region	Number of stations	Minimal size, um	Average filtered volume, m^3	FTIR/Raman, % of items	Abundance, items/m^3	Reference
Atlantic						
NE Atlantic	470	250	2	0.3	2.46	Lusher et al. (2014)
NE and NW Atlantic	23	10	2.6	50	13–501	Enders et al. (2015)
NE and SE Atlantic[a]	76	250	2	100	1.15	Kanhai et al. (2017)
Arctic						
North Pole/Central	13	63	0.07	25	44.3	Ross et al. (2021)
Basin	57	250	2	100	0.7	Kanhai et al. (2018)
Eurasian Arctic	60	100	3.3	100	0.8	Yakushev et al. (2021)
Canadian Arctic	34	63	0.07	33	21.1	Ross et al. (2021)
North Atlantic/Fram	24	63	0.07	50	65.1	Ross et al. (2021)
Fram strait	5	32	0.26	5–100	113–1287	Tekman et al. (2020)
Greenland/Barents Sea[a]	75	250	2	1	2.68	Lusher et al. (2015)
Greenland Sea[b]	7	80	1	100	2.4	Morgana et al. (2018)

[a] included rayon.
[b] without fibres, fragments only.

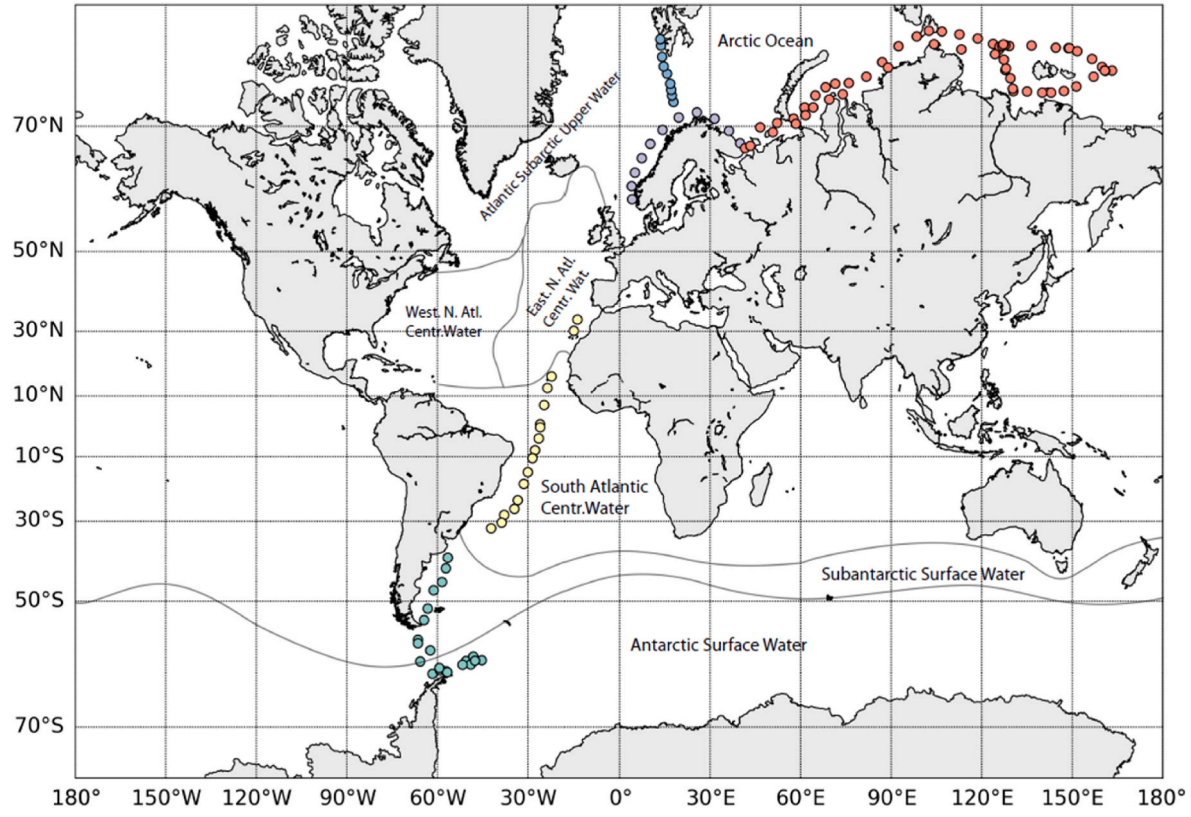

Fig. 1. Location of water sampling positions during the five **research cruises from the Arctic ocean to the Antarctic ocean.** The research cruises are differentiated by coloured positions: cargo vessel Nordbjørn, August 2019 – blue; 78th research cruise of the R/V Akademik Mstislav Keldysh, September–November 2019, leg 1 – red, leg 2 – purple; 79th research cruise of the R/V Akademik Mstislav Keldysh, December 2019–February 2020, leg 1 – yellow, leg 2 – green. Classification of Atlantic Ocean surface water masses according to Emery (2001). (For interpretation of the references to colour in this figure legend, the reader is referred to the Web version of this article.)

was set according to the salinity gradient (Yakushev et al., 2021). In some periods of the year, the water north of Bear Island can be represented by the waters of the Arctic Ocean, which bends around southwestern Spitsbergen, rather than the waters of the North Atlantic Current (Smolyar and Adrov, 2003). In August 2019, four stations near Svalbard had lower salinity and temperature than the other stations along the North Atlantic Current; temperature-salinity data testified different water origins for these stations which was most likely Arctic water (Fig. S1a). These three stations were included in the Barents Sea region. Two stations (the first and the last on the transect Tromsø-Svalbard) were not included in any region as they belong to coastal waters, sampling started/finished inside the fjords.

2.2. Sampling and sample processing

Floating microdebris were collected byfiltering subsurface seawater using ship-board underway pump-through system with an intake located at a depth of about 3 m on the right side of the vessel. This method was implemented following a modified approach of methods applied on different research vessel (Kanhai et al., 2018; Lusher et al., 2015). In order to perform MP sampling, flowing subsurface seawater was passed under pressure through two stainless steel meshes (1.5 mm and 100 μm pore size) within the filtration system, which consisted of two sequentially established first step water appliance protective systems and food grade PVC pipes. A flow meter Decast Metronic BKCM-15/Valtec VLF-U/БЕТАР CXB-15 integrated into the system provided accurate registration of water volume for each sample, which varied from 1 to 8 m^3 per sample (with an average of 3.3 m^3). The system was equipped with a thermosalinograph (*SBE 21 SeaCAT/SBE-911*), which were continuously recording salinity and temperature of flowing subsurface seawater. After every sampling period, collected material was rinsed from the filtration system by backward water flow within the system, and filtered onto stainless steel mesh filters (Ø 25 mm, pore size 50/80 μm) using a filter holder attached directly to the sampling system to avoid contamination from the air. For this purpose, 25 mm filter holders were attached to outlets of the valve of the filtration system. Filters were sealed in pre-rinsed 50–100 mL glass jars or Corning® 50 mL centrifuge tubes rinsed with pre-filtered, 0.45 μm Milli-Q water. These jars/tubes were stored until the analysis in the onshore clean laboratory (NIVA, Oslo). In the laboratory, the samples were processed individually to remove organic matter using an optimized protocol with 10% KOH (24hr incubation at 40° (Bråte et al., 2018)). This was performed in the same jars/tubes where the filters were stored. The processed samples were filtered onto 47 mm GF/A papers with a pore size of 1.6 μm. The filter with material was immediately transferred to a Petri dish and covered for drying and further analysis.

2.3. Microplastics identification

All particles from the water samples (as well as procedural and field blanks) were analysed using a combination of visual inspection and chemical identification of polymeric composition via spectroscopy methods. All samples were visually inspected under stereo microscope (Nikon SMZ745×T, 20 × magnification), measured (at their longest, length and shortest, width, mm, and square, mm^2) and photographed (using Infinity 1–3C/INFINITY 1 Lumenera camera and INFINITY ANALYZE and CAPTURE software). Visual identification followed the methods and standards presented in Lusher et al. (2020) regarding MP categorization by shape, size and colour. Visual identification was confirmed by Fourier Transform Infrared spectroscopy (μFT-IR analysis

on *PerkinElmer Spotlight 400 FTIR; transmission micro-FTIR with a diamond compression cell, DCC)*. Measurements were obtained at 4 cm^{-1} spectral resolution for the range 4000 to 600 cm^{-1}. Library matching was performed in the Spectrum 10 software (v. 10.6.2). Each spectrum was compared to several different libraries available at NIVA: PerkinElmer ATR Polymers library, STJapan Polymers ATR library, BASEMAN library (Primpke et al., 2018), and several in-house libraries including reference polymers, different textile materials, and potential sources of laboratory contamination. All spectra were manually inspected to ensure that the library matches were acceptable. Only synthetic items were included in the dataset for further analysis. Semi-synthetic biobased polymers, and those that can be difficult to separate from natural materials, such as rayon/viscose were excluded. The weight of subsurface MP was estimated based on the polymer density and volume of every particle, with an assumption that all the fibers are cylinders with visible diameter, and the fragments thickness was roughly estimated by comparison with the sizes of the fibers nearby. About 2% of items (fibers only) were lost during analysis under transfer from GF/A filter to DCC. In this case plastic or non-plastic nature of the item was determined by comparing with other fibers on the filter and according to the guidelines for visual identification (Lusher et al., 2020).

2.4. Contamination control

To mitigate sample contamination, several procedural steps were introduced. All equipment and glass jars were rinsed with pre-filtered (0.45 μm) Milli-Q water before use. Filters were checked under a microscope for contamination prior to use. The samples and used equipment were covered where practically possible with aluminium foil or glass to minimise periods of exposure. All consumables were taken directly from their packaging and checked for contamination under a microscope (i.e. GF/A filters). Samples of all consumables were included in the spectra database. Personal protective equipment, 100% cotton lab coats, and gloves were worn during the whole processing procedure. All procedures in the laboratory were conducted in a clean airflow cabinet (Labculture LA2-5A1-E).

To monitor the potential introduction of contamination during the sampling and analysis procedure, field and procedural blanks were introduced. Specifically, sampling field blanks were performed alongside the subsurface sampling procedure (1–3 field blanks per cruise – 1 blank per about 11–20 samples) using the same procedures as for subsurface sampling excluding seawater pumping when filters were in the filtration system. In the laboratory, procedural blanks (3 blanks per 20 samples, 10% KOH in a glass jars) were run simultaneously with the processing of samples. All field and procedural blanks were analysed for MPs in the same way as the samples using a dissecting microscope *Nikon SMZ745* and FTIR after filtering onto GF/A paper.

A total of nine fibers were found in the field blanks (0–3 fibers per blank, 7 blanks), and two fibers in procedural blanks (0–1 fiber per blank, 20 blanks). All fibers detected in the blanks were confirmed as cellulose with the exception of one fiber in a single field blank which was made of Acryl. No similar Acryl fibers (colour, size) were found in any of the remaining blanks or samples. Since all cellulose was excluded from the data set (not presumed to be plastic) and similar Acryl fibers were not observed in any field sample, no data correction was needed. These data and the observation that 23 stations (19%) were free of MP indicate high confidence that MP were not introduced to the samples as a result of contamination during the sampling and processing procedures.

2.5. Statistical analysis

Particle characteristics (morphology, size, weight, polymer type) and metadata on sampling conditions (coordinates, distance to the nearest coast, and volume of filtered water) were compiled in Microsoft Excel. As volumes of water filtered per sample varied, all data were standardized to be presented as either items/m^3 or μg/m^3. All data were processed and visualized using python scientific and graphical packages (*SciPy, Pandas, Matplotlib, Basemap, Q-GIS*). Distances from the coasts for each sampling point were extracted from a global dataset of distances from the nearest coastline of the EarthData online service of NASA.The Pearson correlation matrix was calculated to estimate the possible relationships between the sampling conditions, including distance from the nearest coast, and the measured characteristics of MP. A series of tests were conducted to identify statistically confident differences ($p < 0.05$) among characteristics of MP sampled within different water massesand between the Southern and the Northern Hemispheres. The pairwise Student T-test with Benjamini/Hochberg procedure to control family-wise error rate was applied for numerical parameters. These include the following parameters: abundance of fibers, fragments and total MP, weight concentration, weight of MPand surface area. Anderson-Darling test for k-samples, was used to compare the categorical empirical distributions of polymer type of MP and the Fisher exact test for binary features (MP morphology: fragment or fiber) (Supplementary Material).

3. Results

A total of 121 subsurface water samples were collected over the duration of the five research cruises (Fig. 1), covering a total of transect length of 24,540 km. The total volume of filtered water was 395 m^3 (average per sample – 3.3 ± 1.5 m^3). No statistical correlations between MP characteristics and conditional variables were found (vessel speed, wind speed, temperature, salinity, and filtered volume). From these results, we inferred that the observed differences in MP characteristics were not connected to the changes in the sampling conditions.

MP were found in 81% of the analysed subsurface samples (98/121 samples). A total of 1066 particles were initially isolated during visual identification and only 237 (22%) were confirmed to be plastic by μFT-IR and retained in the dataset for further analysis. This corresponds to between 0 and 7 items per sample. In total, the average abundance of MPs for whole studied area was 0.7 ± 0.6 items/m^3 (ranging from 0 to 2.6 items/m^3), with an equal average abundance for both fragments and fibers (0.34 items/m^3). MP size ranged from 0.1 to 4.9 mm, with an average of 1.1 ± 1.5 mm. MP surface area varied between 0.002 and 1.2 mm^2 (average: 0.1 ± 0.2 mm^2). Average weight concentration was estimated to be 3 ± 8 μg/m^3 (0–69 μg/m^3) (Fig. 5a). Sixteen different polymer types were identified with polyethylene terephthalate (PET, polyester) accounting for 33.0% followed by polymethylmethacrylate (PMMA, acryl) 14.1%, polyethylene (PE) 11.5%, polypropylene (PP) 8.8%, polystyrene (PS) 7.1%, polyamide (PA, nylon) 6.6%, polyvinylchloride (PVC) 4.9%, polytetrafluoroethylene (PTFE) 4.0%, polyurethane (PUR) 3.5%, silicone 1.8%, nitrile butadiene rubber (NBR) 1.8%, polycarbonate (PC) 0.9%, and poly(2,6-diphenyl phenylene oxide) (PPPO), polyoxymethylene (POM), ethylene-propylene, and phenoxy resin accounted for 0.4% each.

3.1. Microplastics characteristics for different ocean regions

The characteristics of MP were used to look for potential differences between the five different ocean regions. The least polluted ocean regions appeared to be the Antarctic and Siberian Arctic with MP absent at 24% and 25% of stations, respectively, which is in line with previous observations (Bagaev et al., 2021). The Barents Sea, North Atlantic and Central Atlantic had between 9% and 12% stations free from MPs.

3.1.1. Abundance

Average MP abundance appeared to be higher in the Barents Sea and Central Atlantic (0.85 and 0.78 items/m^3 respectively) followed by the Siberian Arctic (0.71 items/m^3) and lower abundance – in the North Atlantic and Antarctic regions (0.56 and 0.43 items/m^3 respectively) (Fig. 3a). However, there was no significant difference in average MP abundance between the five studied regions (Table S2). A significant

difference ($p < 0.05$) was found for average MP abundance between the Southern and Northern Hemispheres, 0.47 and 0.77 items/m^3 respectively (Tables S4-S5).

3.1.2. Morphology

The proportion of fibers and fragments across the samples was significantly different between the five ocean regions (Fig. 2b, c and 3b). Fibers accounted for the most abundant particle type in most of the polar regions– 62, 69 and 88% for Siberian Arctic, Antarctic and North Atlantic, respectively. Whilst the Barents Sea was characterized by a higher share of fragments (62%) than fibers. Similarly, fragments were the dominant particle type in the Central Atlantic (94%).

3.1.3. Size

The Central Atlantic and the Barents Sea regions were characterized by the largest sized MP (average surface area 0.18 mm^2 for both regions) followed by the Antarctic region (average 0.08 mm^2) (Fig. 4a). MP items in the North Atlantic and the Siberian Arctic were significantly smaller in size (average 0.03 mm^2). Notably, the size of fibers was significantly higher ($p < 0.05$) in the Southern Hemisphere than in the Northern Hemisphere (average 0.05 and 0.02 mm^2, respectively, Table S5, Fig. 4b). The smallest size of fragments was found in the Siberian Arctic region (average 0.06 mm^2) and the largest - in the Barents Sea and the Central Atlantic (0.25 and 0.20 mm^2, respectively).

3.1.4. Polymer types

The two regions of the Arctic Ocean (the Barents Sea and Siberian Arctic) had a similar polymer composition, which was significantly different from the three regions of the Atlantic Ocean, which also differed from each other (according to the Anderson-Darling test for k-samples, significance level for test value < 0.5%) (Fig. 5a). In the Barents Sea and Siberian Arctic, the most common polymer type was PET/polyester (35 and 38%) followed by PE (19%) in the Barents Sea and PMMA/acryl (21%) in the Siberian Arctic. In the Northern Atlantic, PET/polyester items amounted to 71% and PMMA/acryl – 12%. In the Antarctic region, the two most common polymers were PET/polyester and PA/nylon, accounting for 26% each. Polymer variability in the Central Atlantic differed significantly from the other regions where PE (24%) and PP (21%) were most common. The ratio between the different types of polymers found in the Central Atlantic matched plastic demand in Europe, $R^2 = 0.89$ (Fig. 5b).

3.1.5. Weight concentration

The maximum average weight concentrations of MP were observed in the Barents Sea (7.5 μg/m^3) and the Central Atlantic (7.0 μg/m^3). The lowest were observed in the North Atlantic and Siberian Arctic (0.6 μg/m^3) (Fig. 6b). MP weight concentration in the Barents Sea was characterized by a notable difference between the western and south-eastern parts of the sea, with 10 times higher weight concentrations in the western Barents Sea (Fig. 6a).

4. Discussion

Historically, differences in sampling and analysis applied in MP studies have made it complicated to perform detailed analysis of the results from different regions and studies. As an example, two studies carried out in the same region, with similar methodological approaches in the same year, presented values differing from 0.7 to 40 items per m^3 ((Kanhai et al., 2018; Ross et al., 2021) respectively, Table 1). Level of MP pollution found in this work is in range of previously observed (Table 1).

4.1. Ocean dynamics

The abundance of MP in all oceanic regions investigated in this study appears relatively stable, with no statistically significant difference. The global distribution and similar abundances of MP shown here could suggest that MP inhabiting the subsurface waters have a near neutral buoyancy and became a common feature of the oceanic near-surface waters. We can hypothesize that near neutral buoyancy MP are trapped by turbulent mixing in the upper layer and can be readily redistributed from their sources to distant regions by wind-driven ocean currents, and the Stokes drift associated with surface waves. The subsurface turbulence prevents MP removal from the subsurface part of the water column, unless the process of fragmentation, biofouling or consumption by organisms occur. In contrast, surface MP (which are captured by sampling with surface nets) have positive buoyancy and MP spatial distribution, in addition to currents, is significantly influenced by wind and waves, which can lead to a more sporadic distribution on the ocean surface (Cózar et al., 2017, 2014; Yakushev et al., 2021). This difference in surface and subsurface MP distribution was clearly shown by (Lusher et al., 2015; Yakushev et al., 2021), demonstrating that data collected using both methods could give additional information about MP fate in the World Ocean.

Despite the similar MP abundances, the MP characteristics varied between the studied regions. Differences include size, morphology, polymer types and weight concentration of MP. This suggests that there are different origins of MP across the five regions, as well as fast propagation within the water masses. Three regions of the Atlantic Ocean, belonging to different water masses, had significant differences in the variety of polymer types, morphology, and sizes of MP observed. MP characteristics in two studied regions in the Arctic Ocean differed from those found in the Atlantic Ocean, and had high variability in size and morphology of MP within each region. These two regions can be further divided into five more specific water masses: western and southeastern Barents Sea, high saline Polar water and low saline outer/inner plumes of Siberian rivers which had a large difference in weight concentrations among themselves (Fig. 6; (Yakushev et al., 2021)). Thus, it was shown that the variation in MP characteristics is different for different water masses. This finding agrees with the suggestion presented by Ross et al. (2021) about association of subsurface MP with water masses. In other words, subsurface MP could be used as a tracer for different water masses (Yakushev et al., 2021).

Accumulation zones of surface MP have been identified in the ocean's subtropical gyres (Cózar et al., 2014), although this is not true for MP in subsurface water (Enders et al., 2015). The importance of mesoscale convective flows for subsurface MP distribution has been shown (Vega-Moreno et al., 2021). Although no statistically significant difference in MP abundance across the five ocean regions, some sites were observed to have elevated MP concentrations. The highest MP abundance and weight concentration were found in the Central Atlantic, at stations between 1° S and 18° N (Figs. 2 and 6) where, according to hydrophysical data, equatorial divergence zone and Canary upwelling have been observed (Glukhovets et al., 2021; Fig. S1b). The Central Atlantic region can be used to look for relationships between MP and ocean dynamics - as most stations were located 200 km from the coast, resulting in low influence of coastal sources of MP. From this we can suggest that ocean dynamics is the main factor driving MP distribution here. High MP concentrations were not found in samples of subsurface water near the south Atlantic subtropical gyre, but they were in upwelling areas. Surface MP, sampled in the same cruise, showed an opposite distribution and were found abundant at stations south of 20°S, close to the gyre (Pakhomova et al., 2021), again, emphasizing the difference in the fate of surface and subsurface MP in the global ocean. Convergence and divergence zones appear to be important drivers for elevated concentration of subsurface MP, but not long-term accumulation because of strong seasonal variability of their dynamics. Other stations with maximum MP weight concentration in this study were also observed in regions with active ocean dynamics. For example, near Svalbard where North Atlantic and Arctic waters meet (Figs. 6a and S1a) and in the White Sea Throat which experiences currents from opposite directions, to and from the Barents Sea (Fig. 6a).

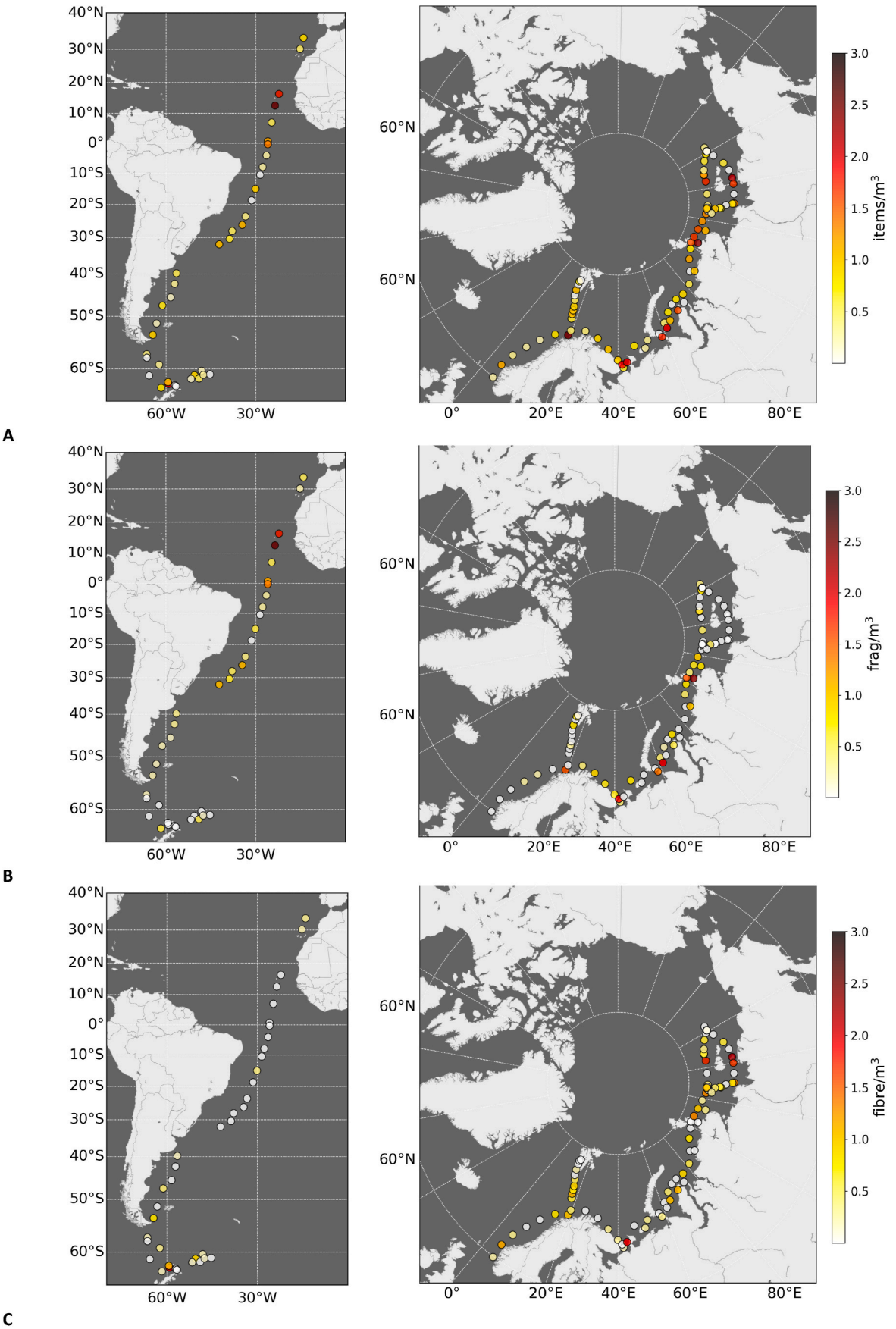

Fig. 2. Abundance of MP at stations, items per m^3: a – total MP, b – fragments only, c – fibers only.

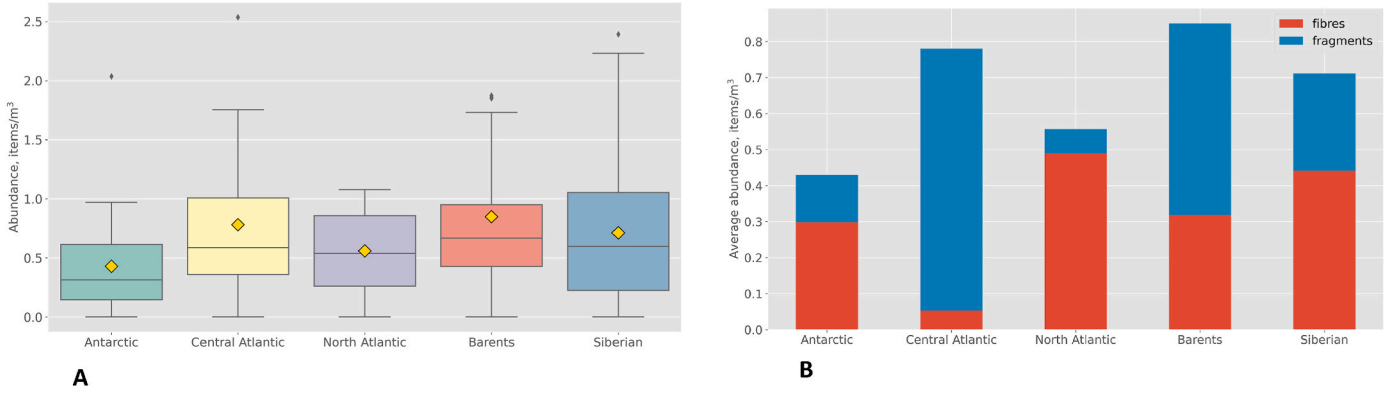

Fig. 3. Abundance of MP for the five different ocean regions, items per m^3: a – boxplots for all found items, b – average abundance of fibers (blue) and fragments (orange). Boxplots display the minimum, the maximum, the first and third quartiles, the sample median (line in the box), and the average (yellow diamond). (For interpretation of the references to colour in this figure legend, the reader is referred to the Web version of this article.)

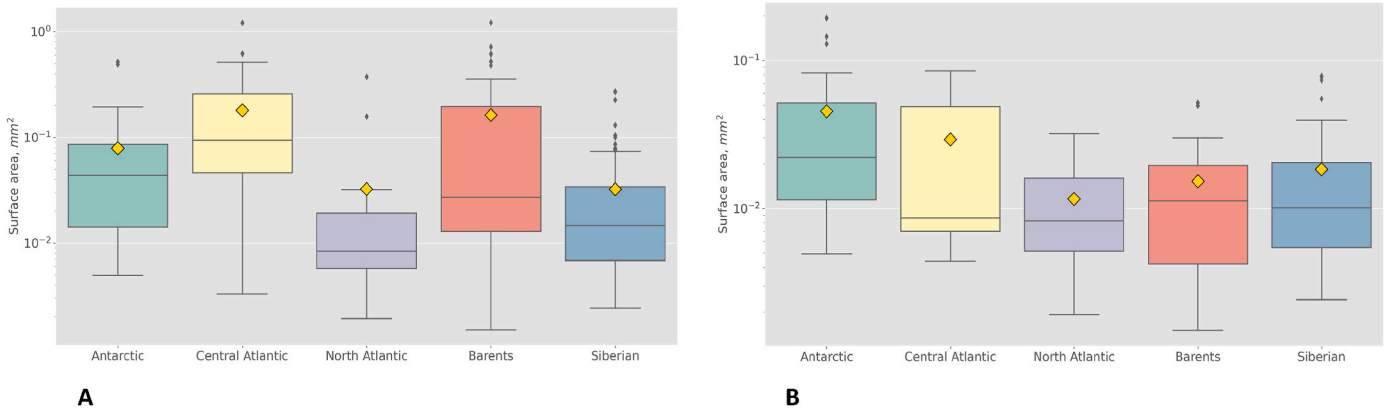

Fig. 4. Surface area of MP (mm^2) for the five different ocean regions: a – all plastic items, b – fibers only.

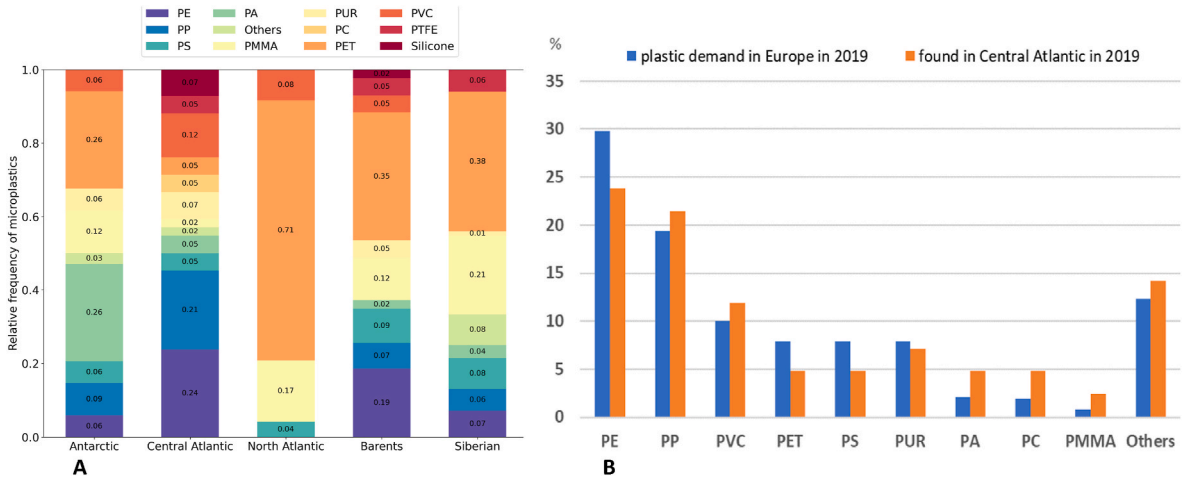

Fig. 5. Polymer types of MP**: a – normalized by number of stations for the five different ocean regions; b – variability of polymer types of MP found in the Central Atlantic (orange) and polymer types demand (blue,** https://www.plasticseurope.org**), R^2 = 0.89.** For (a) – plastic types are listed from the lowest density to the highest density: polyethylene (PE), polypropylene (PP), polystyrene (PS), polyamide (PA), others (nitrile butadiene rubber (NBR), polyoxymethylene (POM), poly(2,6-diphenyl phenylene oxide) (PPPO), ethylene-propylene, and phenoxy resin), polymethyl methacrylate (PMMA, including acryl fibres), polyurethane (PUR), polyethylene terephthalate (PET, including polyester fibres), polyvinyl chloride (PVC), polytetrafluoroethylene (PTFE), silicone. For (b) – others include the same as for (a) along with PTFE and silicone. (For interpretation of the references to colour in this figure legend, the reader is referred to the Web version of this article.)

4.2. Atlantic Ocean

Three regions in the Atlantic Ocean differed significantly from one another. The Antarctic region appeared to be less polluted with MP: it contained the biggest number of stations free from MPand the lowest average abundance of MP. We expected to find less MP in this region as it has a low population density and less intense offshore industries than the other regions. The observed MP are possibly entering the region

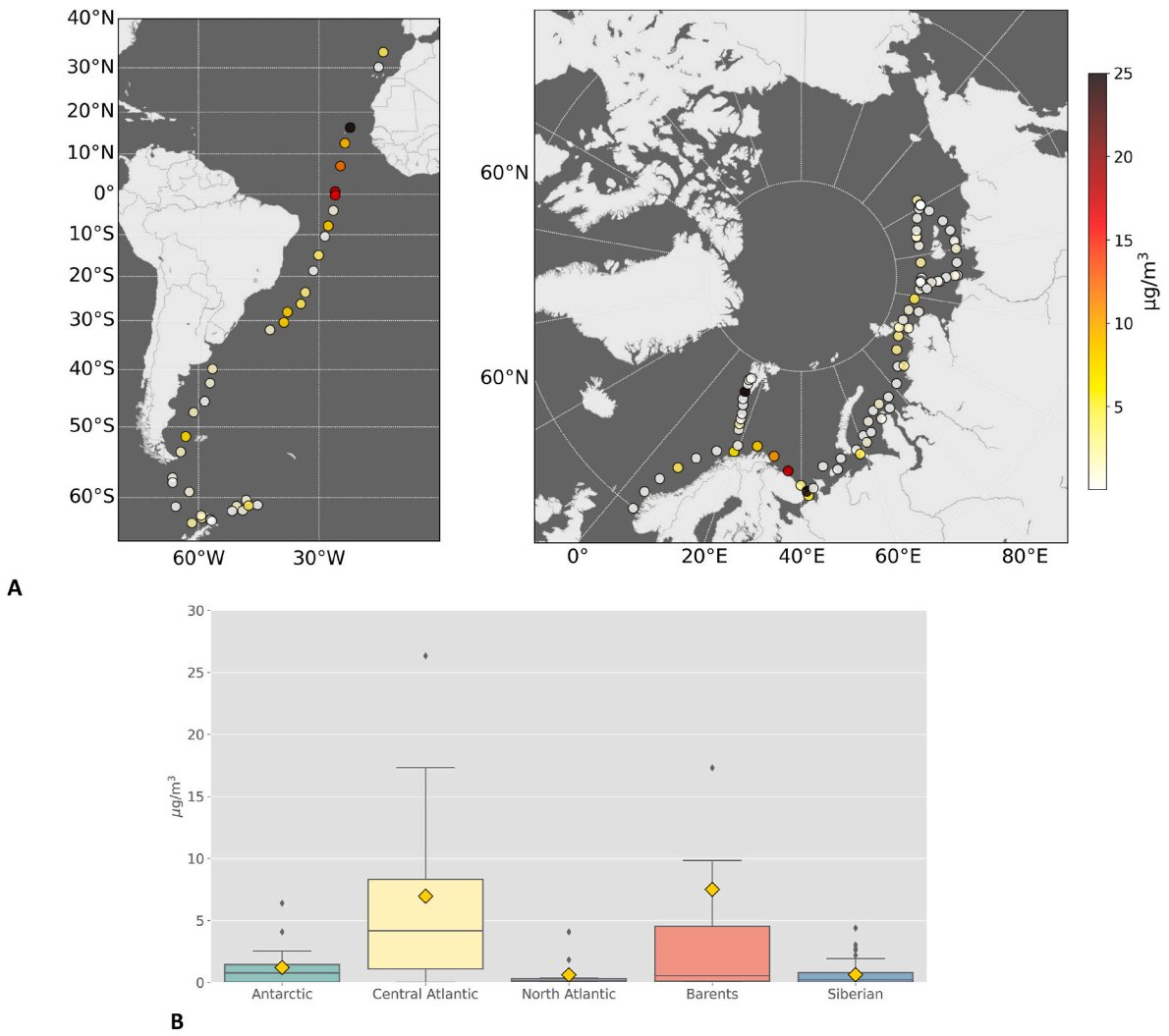

Fig. 6. Weight concentration of MPs, µg/m^3: a – weight concentration at stations, b – boxplots for the five different regions.

because of surface currents, rather than localized input indicating fast spreading of MP through the World Ocean. The fate of MP in the ocean is influenced not only by hydrophysical processes. Physical-chemical degradation and biofouling change the density of particles resulting in increase of sinking rate for light polymers and decrease for dense polymers (Kooi et al., 2017; Kowalski et al., 2016) and thus increasing particle residence time in the water (Lobelle et al., 2021). The region of Antarctic Circumpolar Current is characterized by high primary production that can lead to intensive processes of biofouling and longer residence time of MP particles in the region.

The highest abundance of fragments, the largest MP particles, and the highest weight concentrations in Atlantic Ocean were found in the Central Atlantic. This may indicate a significant role of local sources of MP. As the distance from the coast for most of studied stations was more than 200 km, it is unlikely that coastal sources can be the main source of MP in the Central Antarctic. Some of studied stations here belonged to the latitude of the Amazon river but the river plume spreads mainly to the north during this time of the year, (Glukhovets et al., 2021). It is unlikely that the Amazon river was a source of the observed MP. The subtropical south Atlantic gyre has been identified as a plastic accumulation point (Cózar et al., 2014) which could be contributing to the Central Arctic values observed in this study. All stations in this region - with exception of two northern stations - belong to the same water mass as the south Atlantic gyre. Variability of polymer types found in central Atlantic coincides with the global plastic demand. This points to MP accumulation in the region rather than random dispersal. We can suppose that macroplastic and MP were accumulated in the surface waters of the subtropical gyre following their further fragmentation, biofouling, sinking to the subsurface layer and spreading within the whole water mass.

4.3. Arctic ocean

The Barents Sea had the highest abundance and weight concentrations of MP in the present study. Although it is more difficult to interpret the main source of MP in this region. All stations in the Barents Sea were located within 200 km from the coast and according to salinity, they were represented by both high saline North Atlantic water (34–35 psu) and lower saline coastal water (28–32 psu). It therefore likely that samples in the Barents Sea were influenced by MP discharged in coastal regions. One line of argument follows that the Barents Sea is the most populated region in the Arctic and has high shipping and fishing activity (Schoolmeester, 2018). This suggest that local sources of MP may be dominated by coastal discharge and maritime activity. A second line of argument was presented whereby it was hypothesized that the Barents Sea may be a sixth accumulation zone for plastics and the "dead end" of MPs transport from the North Atlantic (Cózar et al., 2017; Van Sebille et al., 2012). We did not find any signs of high MP pollution from the North Atlantic in this study. The North Atlantic region was the least contaminated with MP of all the studied regions in terms of item size and

weight concentration. However, all stations in this region had MP particles with quite similar characteristics – 88% fibers, small size (average: 0.03 mm^2). Such small size of the items can indicate long residence time in the seawater as well as long-range transport (Ross et al., 2021). Given the conflicting information obtained in our study, it was not possible to draw any conclusions about which of the water bodies was the main driver behind the observed MPs concentrations (and thus short- or long-range sources). Detailed mapping of MP in the whole Barents Sea is needed to understand their fate.

In the studied areas of the Arctic Ocean the maximum MP weight concentration was found in the western Barents Sea whereas the Siberian Arctic was less contaminated with MP. No marked increased in MP pollution in the plumes of the Great Siberian Rivers has previously been observed (Yakushev et al., 2021). Sampling in the Siberian Arctic was carried out in October, in the period of low discharge from these rivers. It is possible that in the flood period, more MP are transported by these rivers to the Arctic while in the autumn period riverine waters decrease MP pollution in the Arctic. One important factor for the Great Siberian Rivers is that only the upstream regions of these rivers are populated, which can be a source of MP pollution. It may be inferred that plastic particles will degrade during transport downstream, sinking to the bottom, or move to the shore. Thus, the main plastic pollution load may remain within the freshwater river systems. We suggest that this is a paradox of Siberian rivers plastic discharge, the rivers do not pollute but dilute the plastic concentration in the Arctic, at least in the Autumn period.

Significant decrease of MP size from the western Barents Sea to the south-eastern Barents Sea and to the Siberian Arctic were observed. This can testify to the MP degradation during transport from the source in the Barents Sea. This coincides with distribution of macroplastics in the same regions, whereby they were only observed in the Barents Sea (Pogojeva et al., 2021). High saline water in the Siberian Arctic (between the Yenisei and Lena rivers) did not contain surface MP but contained subsurface MP with very similar characteristics to those in the south-eastern Barents Sea (Yakushev et al., 2021). This all indicates fast spreading of subsurface MP within one water mass but not at the surface. The main MP pollution in the Siberian Arctic appears to originate in the Barents Sea.

4.4. Comparison of two Hemispheres

Some differences were observed between the two Hemispheres. MP abundance was higher in the Northern Hemisphere compared to the Southern Hemisphere that was driven by fiber abundance ($p < 0.05$, Tables S4-S5, Fig. 2b). When considering all fibers, both synthetic, semi-synthetic and non-synthetic, their abundance in the Southern Hemisphere was 3.5 times lower than in the Northern Hemisphere ($p < 0.05$, Table S4-S5, Fig. 7). Fibers in the Southern Hemisphere were longer and wider than those observed in the Northern Hemisphere (average 0.05 and 0.02 mm^2, respectively; Fig. 4b), this may indicate shorter residence time in the seawater and higher influence of local source, i.e. maritime activity. In the Northern Hemisphere, the most abundant items were polyester fibers, 35–71%, followed by acryl fibers, 12–21%. Clothing/textiles are potential sources of polyester and acrylic fibers, as various fabrics can release fibers during the laundry process (Carney Almroth et al., 2018; De Falco et al., 2019; Napper and Thompson, 2016) resulting in dominance of synthetic fibers in municipal wastewater (Sun et al., 2019). These fibers can escape wastewater treatment processes, release into coastal waters and readily disperse into the open ocean (Covernton et al., 2019; Karcher et al., 2012; Smith et al., 2011). Nylon items are often associated with maritime activities (e.g., fishing nets), these were less abundant in the Northern Hemisphere, 0–4% (Fig. 5a). The Southern Hemisphere, i.e. Antarctic region, differed significantly from the regions in the Northern hemisphere, the most common polymer types were polyester and nylon, 26% each. Summarizing differences found in fiber's abundance, size and types we can conclude that the Northern Hemisphere is more polluted with plastic from the coastal discharge than the Southern Hemisphere, where maritime activity plays an important role in MP pollution. This could be a result of the difference in population for two Hemispheres – the Northern Hemisphere is home to approximately 88% of the earth's total human population ("World Population Review," n.d.), which corresponds to a higher consumption of textile fibers ("Chemical Economical Handbook," n.d.) and consequently, higher release to the environment.

4.5. Dependence on distance from the coast and the latitude

As terrestrial input is one of the main sources of MP to seawater, the distance from the coast should be an important factor surrounding MP distirbution. Our data showed that the closer to the shore, the higher the abundance of fibers, which were also found at more stations (Table S1), $R^2 = -0.29$. The correlation could not be very high because there are other factors influencing the transport of fibers, and there are local sources of MP, which have high variability. No trend was found between abundance and distance from the coast for the fragments (Table S1). This could indicate different fate of fragments and fibers in the seawater. Size of fragments is very important for existing in the subsurface layer. Most fragments observed in this study were less than 1 mm in length, median 0.5 mm, 25th-75th persentile 0.3-0.9 mm. Larger-sized and light polymers, with a density lower than seawater (PE, PP, expanded PS and

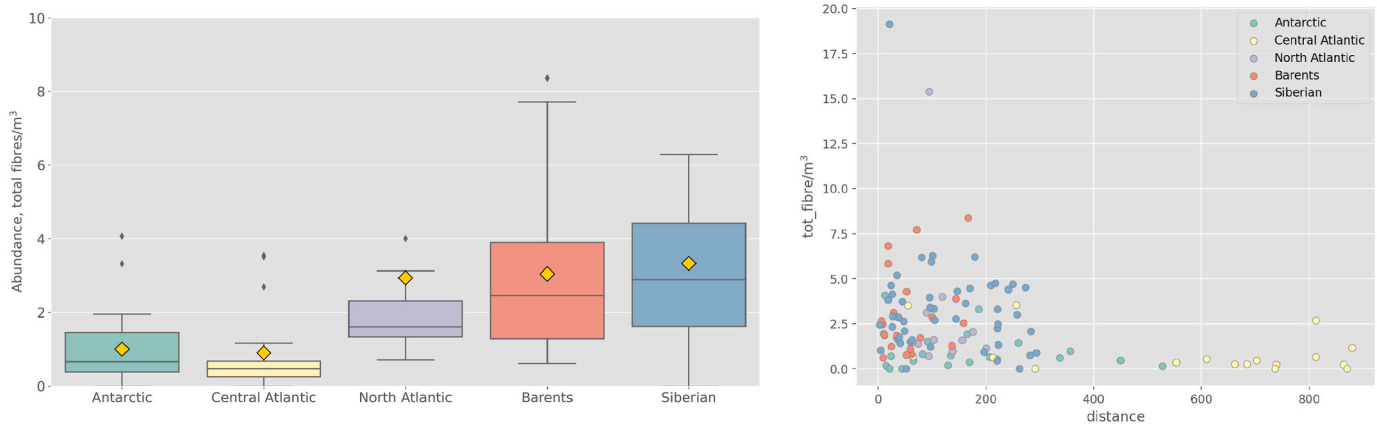

Fig. 7. Variability of all found fibers (synthetic, semi-synthetic and non-synthetic, items/m^3): a – abundance for the five different ocean regions, boxplots; b – abundance at each station plotted against distance from the coast (km).

PUR foam), are usually found floating at the surface (Yakushev et al., 2021), while larged-sized and more dense polymers (PVC, PET, PS, PA, etc.) were rarely found floating. It is assumed that they sink quickly to the bottom after entering the ocean. Particles less than 200 μm in size do not reside in seawater for long as the processes of fragmentation and biofouling can lead to changes in particle size and properties, removing them from the subsurface water at a faster rate than larger-sized fragments (Enders et al., 2015; Lobelle et al., 2021). It appears that only fragments of a certain size range can exist in the subsurface layer and for a limited time, which restricts their spread to close proximity from their source, and probably within the same water mass.

The highest abundance of fibers and proportion of fibers was found in the North Atlantic, Antarctic and in the Siberian Arctic, where the latter are less populated regions. This can indicate that fibers have longer residence time in subsurface water and/or can be transported for longer distance than fragments. Maximum fiber abundance in the Polar regions and absence of fibers in the Central Atlantic can testify to different mechanisms of transport for fragments and fibers. It is known that atmospheric transport is very important for the delivery of fine particulate matter to remote regions. In equatorial/tropic regions, 30° N-30° S, warm rising air prevents a deposition of airborn particles to the ocean. While in polar regions, >60°, cold descending air encourages airborne particles to fall out. These features of global atmospheric circulation result in polar regions being more polluted with atmospheric contaminants. A significant number of studies have demonstrated long-range transport of air pollution to the Arctic (Law et al., 2014; Law and Stohl, 2007; Odland et al., 2016). The same mechanism was also supposed for MPs, especially for the lower size fraction (Allen et al., 2019; Bergmann et al., 2019; Dris et al., 2016; Evangeliou et al., 2020). Our results support this assumption for fibers (Fig. 8). Correlation between abundance of fibers and latitude amounted to 0.29.

The spatial distribution of our stations was mostly restricted to within 300 km from the coast, with most of the stations found in the Northern Hemisphere north to 60N (Figure 1, 7 and 8). Therefore, our data does not allow to make statistically confirmed conclusions about global features of MP distribution. Moreover, distribution of subsurface MP could have temporal variability as its sources (riverine input), transport (ocean dynamics, biofouling) and consumption (zooplankton, fish) have seasonality. However, our results indicated that distribution of fibers depends on both distance from the coast and latitude, and fibers can be transported for long distance with air and water from the source, while distribution of fragments is limited mainly to the water mass where the source is located.

5. Conclusions

In this study we have used the same methods from sample collection to data reporting to obtain data on MP in subsurface waters covering a wide area of the World Ocean: from the Eurasian Arctic seas through the Atlantic Ocean, and to the Antarctic Peninsula. MP were found in all studied regions showing similar range of MP abundance, but different weight concentrations. These results suggest that MP inhabiting the subsurface waters became a common feature of the oceanic near-surface layer driven by ocean dynamics, while there may be different sources of MP in each region. The most polluted regions were the Central Atlantic and the Barents Sea. Our data indicate that the Barents Sea is the main source of MP in the Siberian Arctic. MP fiber abundance in the Northern Hemisphere is about 2 times higher than in the Southern Hemisphere (3.5 for all found fibers). This is inline with the distribution of the global population density. A relationship between abundance and distance to shore, and latitude was found for fibers but not for fragments, indicating difference in their fate in the ocean.

Research data

All data used in the paper are presented on the figures.

Author contributions

E.Y., B.v.B., S.P. designed and coordinated the study; E.Y., A.B., K.S.

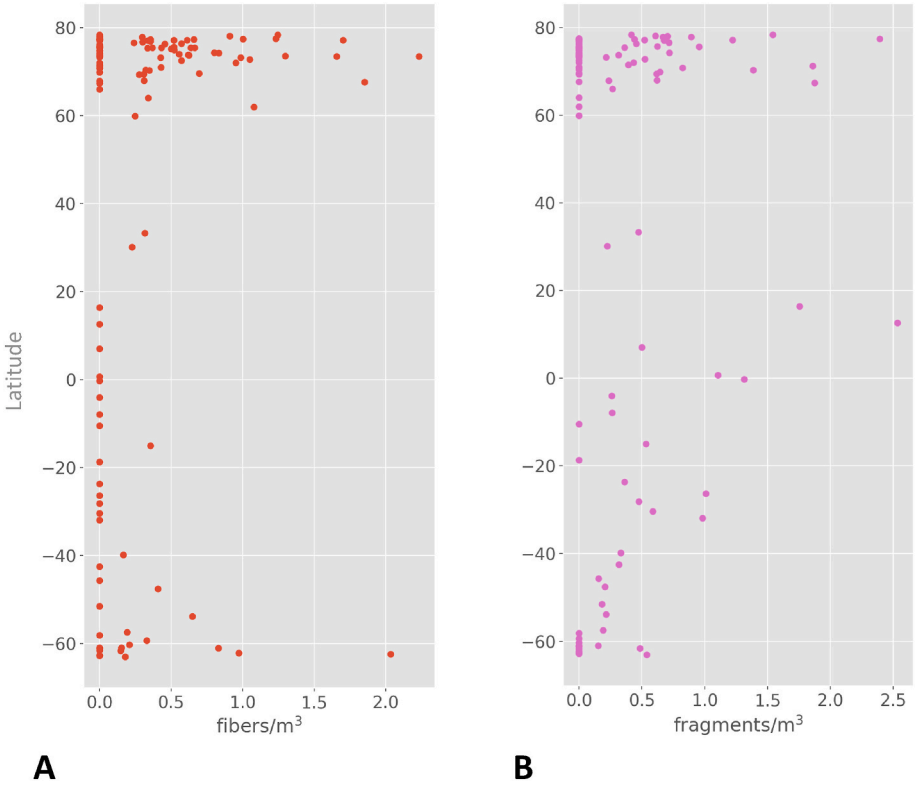

Fig. 8. Abundance of fibers (a) and fragments (b) collected across different latitudes.

conducted field work and collected the samples; S.P., A.B., I.Z. processed the samples and conducted data analyses; S.P., E.Y., A.B., I.Z., K.S., A.L., B.v.B., O.Z. wrote the article. All authors reviewed and commented on the final version.

Declaration of competing interest

The authors declare that they have no known competing financial interests or personal relationships that could have appeared to influence the work reported in this paper.

Acknowledgements

This work was partly funded by the Norwegian Ministry of Climate and Environment projects RUS-19/0001 "Establish regional capacity to measure and model the distribution and input of microplastics to the Barents Sea from rivers and currents (ESCIMO)", and "Model-based mapping of marine litter and microplastic in the Barents Sea (MAMBA)". S.P., A.B, I.Z., K.S., P.Z., and E.Y. were funded by the Ministry of Science and Higher Education of Russia. A.B, I.Z., P.Z. and E.Y. were funded by the Russian Foundation for Basic Research according to the research projects 19-55-80004, 20-35-90056. E.Y. was supported by the Russian Science Foundation Grant 21-77-30001. A.L. and B.v.B received funding from the European Union's Horizon 2020 Coordination and Support Action program under grant agreement No 101003805. The authors are grateful to Oleg Dudarev, Vladimir Rogozhin, Denis Kosmach, Eduard Spivak, Maria Kapustina and Natalia Stepanova for assistance during samples collecting, Cecilie Singdahl-Larsen for assistance with sample analysis, Alexander Osadchiev and Igor Semiletov for supportive discussions, and the captain and crew of R/V Akademik Mstislav Keldysh for facilitating the survey.

Appendix A. Supplementary data

Supplementary data to this article can be found online at https://doi.org/10.1016/j.envpol.2022.118808.

References

Allen, S., Allen, D., Phoenix, V.R., Le Roux, G., Durántez Jiménez, P., Simonneau, A., Binet, S., Galop, D., 2019. Atmospheric transport and deposition of microplastics in a remote mountain catchment. Nat. Geosci. 12, 339–344. https://doi.org/10.1038/s41561-019-0335-5.

Bagaev, A., Esiukova, E., Litvinyuk, D., Chubarenko, I., Veerasingam, S., Venkatachalapathy, R., Verzhevskaya, L., 2021. Investigations of plastic contamination of seawater, marine and coastal sediments in the Russian seas: a review. Environ. Sci. Pollut. Res. https://doi.org/10.1007/s11356-021-14183-z, 2030.

Berezina, A., Yakushev, E., Savchuk, O., Vogelsang, C., Staalstrom, A., 2021. Modelling the influence from biota and organic matter on the transport dynamics of microplastics in the water column and bottom sediments in the Oslo Fjord. Water 13, 2690. https://doi.org/10.3390/w13192690.

Bergmann, M., Mützel, S., Primpke, S., Tekman, M.B., Trachsel, J., Gerdts, G., 2019. White and wonderful? Microplastics prevail in snow from the Alps to the Arctic. Sci. Adv. 5, 16–18. https://doi.org/10.1126/sciadv.aax1157.

Brander, S.M., Renick, V.C., Foley, M.M., Steele, C., Woo, M., Lusher, A., Carr, S., Helm, P., Box, C., Cherniak, S., Andrews, R.C., Rochman, C.M., 2020. Sampling and quality assurance and quality control: a guide for scientists investigating the occurrence of microplastics across matrices. Appl. Spectrosc. 74, 1099–1125. https://doi.org/10.1177/0003702820945713.

Bråte, I.L.N., Hurley, R., Iversen, K., Beyer, J., Thomas, K.V., Steindal, C.C., Green, N.W., Olsen, M., Lusher, A., 2018. Mytilus spp. as sentinels for monitoring microplastic pollution in Norwegian coastal waters: a qualitative and quantitative study. Environ. Pollut. 243, 383–393. https://doi.org/10.1016/j.envpol.2018.08.077.

Campos da Rocha, F.O., Martinez, S.T., Campos, V.P., da Rocha, G.O., de Andrade, J.B., 2021. Microplastic pollution in Southern Atlantic marine waters: review of current trends, sources, and perspectives. Sci. Total Environ. 782, 146541. https://doi.org/10.1016/j.scitotenv.2021.146541.

Carney Almroth, B.M., Åström, L., Roslund, S., Petersson, H., Johansson, M., Persson, N. K., 2018. Quantifying shedding of synthetic fibers from textiles; a source of microplastics released into the environment. Environ. Sci. Pollut. Res. 25, 1191–1199. https://doi.org/10.1007/s11356-017-0528-7.

Chemical Economical Handbook [WWW Document], n.d. URL Polyester Fibers% 0AChemical Economics Handbook.

Chubarenko, I., Esiukova, E., Bagaev, A., Isachenko, I., Demchenko, N., Zobkov, M., Efimova, I., Bagaeva, M., Khatmullina, L., 2018. Behavior of Microplastics in Coastal Zones, Microplastic Contamination in Aquatic Environments: an Emerging Matter of Environmental Urgency. Elsevier Inc. https://doi.org/10.1016/B978-0-12-813747-5.00006-0.

Covernton, G.A., Pearce, C.M., Gurney-Smith, H.J., Chastain, S.G., Ross, P.S., Dower, J. F., Dudas, S.E., 2019. Size and shape matter: a preliminary analysis of microplastic sampling technique in seawater studies with implications for ecological risk assessment. Sci. Total Environ. 667, 124–132. https://doi.org/10.1016/j.scitotenv.2019.02.346.

Cowger, W., Booth, A.M., Hamilton, B.M., Thaysen, C., Primpke, S., Munno, K., Lusher, A.L., Dehaut, A., Vaz, V.P., Liboiron, M., Devriese, L.I., Hermabessiere, L., Rochman, C., Athey, S.N., Lynch, J.M., De Frond, H., Gray, A., Jones, O.A.H., Brander, S., Steele, C., Moore, S., Sanchez, A., Nel, H., 2020. Reporting guidelines to increase the reproducibility and comparability of research on microplastics. Appl. Spectrosc. 74, 1066–1077. https://doi.org/10.1177/0003702820930292.

Cózar, A., Echevarría, F., González-Gordillo, J.I., Irigoien, X., Úbeda, B., Hernández-León, S., Palma, Á.T., Navarro, S., García-de-Lomas, J., Ruiz, A., Fernández-de-Puelles, M.L., Duarte, C.M., 2014. Plastic debris in the open ocean. Proc. Natl. Acad. Sci. U. S. A. 111, 10239–10244. https://doi.org/10.1073/pnas.1314705111.

Cózar, A., Martí, E., Duarte, C.M., García-de-Lomas, J., Van Sebille, E., Ballatore, T.J., Eguíluz, V.M., Ignacio González-Gordillo, J., Pedrotti, M.L., Echevarría, F., Troublè, R., Irigoien, X., 2017. The Arctic ocean as a dead end for floating plastics in the north Atlantic branch of the thermohaline circulation. Sci. Adv. 3, 1–9. https://doi.org/10.1126/sciadv.1600582.

De Falco, F., Di Pace, E., Cocca, M., Avella, M., 2019. The contribution of washing processes of synthetic clothes to microplastic pollution. Sci. Rep. 9, 1–11. https://doi.org/10.1038/s41598-019-43023-x.

Dris, R., Gasperi, J., Saad, M., Mirande, C., Tassin, B., 2016. Synthetic fibers in atmospheric fallout: a source of microplastics in the environment? Mar. Pollut. Bull. 104, 290–293. https://doi.org/10.1016/j.marpolbul.2016.01.006.

Emery, W.J., 2001. Water types and water masses. Encycl. Ocean Sci. 3179–3187. https://doi.org/10.1006/rwos.2001.0108.

Enders, K., Lenz, R., Stedmon, C.A., Nielsen, T.G., 2015. Abundance, size and polymer composition of marine microplastics ≥10 μm in the Atlantic Ocean and their modelled vertical distribution. Mar. Pollut. Bull. 100, 70–81. https://doi.org/10.1016/j.marpolbul.2015.09.027.

Eriksen, M., Lebreton, L.C.M., Carson, H.S., Thiel, M., Moore, C.J., Borerro, J.C., Galgani, F., Ryan, P.G., Reisser, J., 2014. Plastic pollution in the world's oceans: more than 5 trillion plastic pieces weighing over 250,000 tons afloat at sea. PLoS One 9, 1–15. https://doi.org/10.1371/journal.pone.0111913.

Evangeliou, N., Grythe, H., Klimont, Z., Heyes, C., Eckhardt, S., Lopez-Aparicio, S., Stohl, A., 2020. Atmospheric transport is a major pathway of microplastics to remote regions. Nat. Commun. 11 https://doi.org/10.1038/s41467-020-17201-9.

GESAMP, 2019. Guidelines for the monitoring and assessment of plastic litter in the ocean. In: Kershaw, P.J., Turra, A., Galgani, F. (Eds.), IMO/FAO/UNESCO-IOC/UNIDO/WMO/IAEA/UN/UNEP/UNDP/ISA Joint Group of Experts on the Scientific Aspects of Marine Environmental Prote. Rep. Stud. GESAMP, vol. 99, p. 130p.

Glukhovets, D.I., Salyuk, P.A., Artemiev, V.A., Shtraikhert, E.A., Zakharkov, S.P., 2021. Variability of bio-optical characteristics of surface water layer during transatlantic transect in 2019–2020 //. Oceanology 61 (6), 872–880.

Isobe, A., Azuma, T., Cordova, M.R., Cózar, A., Galgani, F., Hagita, R., Kanhai, L.D., Imai, K., Iwasaki, S., Kako, S., Kozlovskii, N., Lusher, A.L., Mason, S.A., Michida, Y., Mituhasi, T., Morii, Y., Mukai, T., Popova, A., Shimizu, K., Tokai, T., Uchida, K., Yagi, M., Zhang, W., 2021. A multilevel dataset of microplastic abundance in the world's upper ocean and the Laurentian Great Lakes. Microplast. Nanoplast. 1, 16. https://doi.org/10.1186/s43591-021-00013-z.

Kanhai, L.D.K., Gårdfeldt, K., Lyashevska, O., Hassellöv, M., Thompson, R.C., O'Connor, I., 2018. Microplastics in sub-surface waters of the Arctic central basin. Mar. Pollut. Bull. 130, 8–18. https://doi.org/10.1016/j.marpolbul.2018.03.011.

Kanhai, L.D.K., Officer, R., Lyashevska, O., Thompson, R.C., O'Connor, I., 2017. Microplastic abundance, distribution and composition along a latitudinal gradient in the Atlantic Ocean. Mar. Pollut. Bull. 115, 307–314. https://doi.org/10.1016/j.marpolbul.2016.12.025.

Karcher, M., Smith, J.N., Kauker, F., Gerdes, R., Smethie, W.M., 2012. Recent changes in Arctic Ocean circulation revealed by iodine-129 observations and modeling. J. Geophys. Res. Ocean. 117, 1–17. https://doi.org/10.1029/2011JC007513.

Kooi, M., Van Nes, E.H., Scheffer, M., Koelmans, A.A., 2017. Ups and downs in the ocean: effects of biofouling on vertical transport of microplastics. Environ. Sci. Technol. 51, 7963–7971. https://doi.org/10.1021/acs.est.6b04702.

Kowalski, N., Reichardt, A.M., Waniek, J.J., 2016. Sinking rates of microplastics and potential implications of their alteration by physical, biological, and chemical factors. Mar. Pollut. Bull. 109, 310–319. https://doi.org/10.1016/j.marpolbul.2016.05.064.

Law, K.L., Morét-Ferguson, S., Maximenko, N.A., Proskurowski, G., Peacock, E.E., Hafner, J., Reddy, C.M., 2010. Plastic accumulation in the North Atlantic subtropical gyre. Science (80- 329, 1185–1188. https://doi.org/10.1126/science.1192321.

Law, K.S., Stohl, A., 2007. Arctic air pollution: origins and impacts. Science 315 (80), 1537–1540. https://doi.org/10.1126/science.1137695.

Law, K.S., Stohl, A., Quinn, P.K., Brock, C.A., Burkhart, J.F., Paris, J.D., Ancellet, G., Singh, H.B., Roiger, A., Schlager, H., Dibb, J., Jacob, D.J., Arnold, S.R., Pelon, J., Thomas, J.L., 2014. Arctic air pollution: new insights from POLARCAT-IPY. Bull. Am. Meteorol. Soc. 95, 1873–1895. https://doi.org/10.1175/BAMS-D-13-00017.1.

Lobelle, D., Kooi, M., Koelmans, A.A., Laufkötter, C., Jongedijk, C.E., Kehl, C., van Sebille, E., 2021. Global modeled sinking characteristics of biofouled microplastic. J. Geophys. Res. Ocean. https://doi.org/10.1029/2020jc017098.

Lusher, A.L., Burke, A., O'Connor, I., Officer, R., 2014. Microplastic pollution in the Northeast Atlantic Ocean: validated and opportunistic sampling. Mar. Pollut. Bull. 88, 325–333. https://doi.org/10.1016/j.marpolbul.2014.08.023.

Lusher, A.L., Munno, K., Hermabessiere, L., Carr, S., 2020. Isolation and Extraction of Microplastics from Environmental Samples: An Evaluation of Practical Approaches and Recommendations for Further Harmonization. Applied Spectroscopy 74 (9), 1049–1065. https://doi.org/10.1177/0003702820938993.

Lusher, A.L., Tirelli, V., O'Connor, I., Officer, R., 2015. Microplastics in Arctic polar waters: the first reported values of particles in surface and sub-surface samples. Sci. Rep. 5, 1–9. https://doi.org/10.1038/srep14947.

Michida, Y., Chavanich, S., Chiba, S., Cordova, M.R., Cózar, C.A., Galgani, F., Hagmann, P., Hinata, H., Isobe, A., Kershaw, P., Kozlovskii, N., Li, D., Lusher, A.L., Marti, E., Mason, S.A., Mu, J.L., Saito, H., Shim, W.J., Syakti, A.D., Takada, H., Thompson, R., Tokai, T., Uchida, K., Wang, J., 2019. Guidelines for harmonizing ocean surface microplastic. Guidel. Harmon. Ocean Surf. Microplastic Monit. Methods 71.

Moore, C.J., 2008. Synthetic polymers in the marine environment: A rapidly increasing, long-term threat. Environ. Res. 108, 131–139. https://doi.org/10.1016/j.envres.2008.07.025.

Morgana, S., Ghigliotti, L., Estévez-Calvar, N., Stifanese, R., Wieckzorek, A., Doyle, T., Christiansen, J.S., Faimali, M., Garaventa, F., 2018. Microplastics in the Arctic: a case study with sub-surface water and fish samples off Northeast Greenland. Environ. Pollut. 242, 1078–1086. https://doi.org/10.1016/j.envpol.2018.08.001.

Napper, I.E., Thompson, R.C., 2016. Release of synthetic microplastic plastic fibres from domestic washing machines: effects of fabric type and washing conditions. Mar. Pollut. Bull. 112, 39–45. https://doi.org/10.1016/j.marpolbul.2016.09.025.

O'Conchubhair, D., Fitzhenry, D., Lusher, A., King, A.L., Van Emmerik, T., Lebreton, L., Ricaurte-Villota, C., Espinosa, L., O'Rourke, E., 2019. Joint effort among research infrastructures to quantify the impact of plastic debris in the ocean. Environ. Res. Lett. 14 https://doi.org/10.1088/1748-9326/ab17ed.

Odland, J.Ø., Donaldson, S., Dudarev, A.A., Carlsen, A., 2016. AMAP assessment 2015: human health in the Arctic. Int. J. Circumpolar Health 75, 33949. https://doi.org/10.3402/ijch.v75.33949.

Pakhomova, S., Silvestrova, K., Berezina, A., Stepanova, N., Yakushev, E., 2021. Geology of seas and oceans: Proceedings of XXIV International Conference on Marine Geology. Vol. I., in: Geology of Seas and Oceans: Proceedings of XXIV International Conference on Marine Geology, Vol. I.. Shirshov Institute of Oceanology Publishing House, Russian Academy of Sciences, pp. 311–315. https://doi.org/10.29006/978-5-6045110-4-6.

Pogojeva, M., Zhdanov, I., Berezina, A., Lapenkov, A., Kosmach, D., Osadchiev, A., Hanke, G., Semiletov, I., Yakushev, E., 2021. Distribution of floating marine macro-litter in relation to oceanographic characteristics in the Russian Arctic Seas. Mar. Pollut. Bull. 166, 112201. https://doi.org/10.1016/j.marpolbul.2021.112201.

Primpke, S., Wirth, M., Lorenz, C., Gerdts, G., 2018. Reference database design for the automated analysis of microplastic samples based on Fourier transform infrared (FTIR) spectroscopy. Anal. Bioanal. Chem. 410, 5131–5141. https://doi.org/10.1007/s00216-018-1156-x.

Provencher, J.F., Covernton, G.A., Moore, R.C., Horn, D.A., Conkle, J.L., Lusher, A.L., 2020. Proceed with caution: the need to raise the publication bar for microplastics research. Sci. Total Environ. 748, 141426. https://doi.org/10.1016/j.scitotenv.2020.141426.

Ross, P.S., Chastain, S., Vassilenko, E., Etemadifar, A., Zimmermann, S., Quesnel, S.A., Eert, J., Solomon, E., Patankar, S., Posacka, A.M., Williams, B., 2021. Pervasive distribution of polyester fibres in the Arctic Ocean is driven by Atlantic inputs. Nat. Commun. 12, 4–12. https://doi.org/10.1038/s41467-020-20347-1.

Rudels, B., 1989. The formation of polar surface water, the ice export and the exchanges through the Fram Strait. Prog. Oceanogr. 22, 205–248. https://doi.org/10.1016/0079-6611(89)90013-X.

Rudels, B., Jones, E.P., Schauer, U., Eriksson, P., 2004. Atlantic sources of the Arctic Ocean surface and halocline waters. Polar Res. 23, 181–208. https://doi.org/10.1111/j.1751-8369.2004.tb00007.x.

Schoolmeester, T., 2018. Global Linkages: a graphic look at the changing Arctic. In: The Southeast Asia Connection. Berghahn Books, pp. 43–76. https://doi.org/10.2307/j.ctvw04kg7.7.

Sebille, E. Van, Aliani, S., Law, K.L., Maximenko, N., Alsina, J.M., Bagaev, A., Bergmann, M., Chapron, B., Chubarenko, I., Cózar, A., 2020. The Physical Oceanography of the Transport of Fl Oating Marine Debris.

Smith, J.N., McLaughlin, F.A., Smethie, W.M., Moran, S.B., Lepore, K., 2011. Iodine-129, 137Cs, and CFC-11 tracer transit time distributions in the Arctic Ocean. J. Geophys. Res. Ocean. 116, 1–19. https://doi.org/10.1029/2010JC006471.

Smolyar, I., Adrov, N., 2003. The quantitative definition of the Barents Sea Atlantic Water: mapping of the annual climatic cycle and interannual variability. ICES J. Mar. Sci. 60, 836–845. https://doi.org/10.1016/S1054-3139(03)00071-7.

Sun, J., Dai, X., Wang, Q., van Loosdrecht, M.C.M., Ni, B.J., 2019. Microplastics in wastewater treatment plants: detection, occurrence and removal. Water Res. 152, 21–37. https://doi.org/10.1016/j.watres.2018.12.050.

Tekman, M.B., Wekerle, C., Lorenz, C., Primpke, S., Hasemann, C., Gerdts, G., Bergmann, M., 2020. Tying up loose ends of microplastic pollution in the Arctic: distribution from the sea surface through the water column to deep-sea sediments at the HAUSGARTEN observatory. Environ. Sci. Technol. 54, 4079–4090. https://doi.org/10.1021/acs.est.9b06981.

Van Sebille, E., England, M.H., Froyland, G., 2012. Origin, dynamics and evolution of ocean garbage patches from observed surface drifters. Environ. Res. Lett. 7 https://doi.org/10.1088/1748-9326/7/4/044040.

Van Sebille, E., Wilcox, C., Lebreton, L., Maximenko, N., Hardesty, B.D., Van Franeker, J. A., Eriksen, M., Siegel, D., Galgani, F., Law, K.L., 2015. A global inventory of small floating plastic debris. Environ. Res. Lett. 10 https://doi.org/10.1088/1748-9326/10/12/124006.

Vega-Moreno, D., Abaroa-Pérez, B., Rein-Loring, P.D., Presas-Navarro, C., Fraile-Nuez, E., Machín, F., 2021. Distribution and transport of microplastics in the upper 1150 m of the water column at the Eastern North Atlantic subtropical gyre, canary islands, Spain. Sci. Total Environ. 788, 147802. https://doi.org/10.1016/j.scitotenv.2021.147802.

World Population Review [WWW Document], n.d. https://worldpopulationreview.com/.

Yakushev, E., Gebruk, A., Osadchiev, A., Pakhomova, S., Lusher, A., Berezina, A., van Bavel, B., Vorozheikina, E., Chernykh, D., Kolbasova, G., Razgon, I., Semiletov, I., 2021. Microplastics distribution in the Eurasian Arctic is affected by Atlantic waters and Siberian rivers. Commun. Earth Environ. 2, 1–11. https://doi.org/10.1038/s43247-021-00091-0.